International Journal of Materials Science and Applications
2022; 11(3): 66-75
http://www.sciencepublishinggroup.com/j/ijmsa
doi: 10.11648/j.ijmsa.20221103.12
ISSN: 2327-2635 (Print); ISSN: 2327-2643 (Online)

A Sustainable Approach for the Recovery of Manganese from Spent Lithium-Ion Batteries via Photocatalytic Oxidation

Eva Gerold*, Helmut Antrekowitsch

Nonferrous Metallurgy, Montanuniversitaet Leoben, Leoben, Austria

Email address:
eva.gerold@unileoben.ac.at (Eva Gerold), helmut.antrekowitsch@unileoben.ac.at (Helmut Antrekowitsch)
*Corresponding author

To cite this article:
Eva Gerold, Helmut Antrekowitsch. A Sustainable Approach for the Recovery of Manganese from Spent Lithium-Ion Batteries via Photocatalytic Oxidation. *International Journal of Materials Science and Applications*. Vol. 11, No. 3, 2022, pp. 66-75.
doi: 10.11648/j.ijmsa.20221103.12

Received: July 25, 2022; **Accepted**: August 9, 2022; **Published**: August 29, 2022

Abstract: The need to recycle critical materials from spent lithium-ion batteries is undisputed. However, non-critical and currently low-cost elements such as manganese are often neglected. Looking at the development of this technology, however, it is evident that the demand for high-purity manganese for battery production will also increase enormously. The tendency towards active materials with higher manganese contents leads to the conclusion that this element should already be taken into consideration at this stage of the development of recycling processes. This evolution is based on the lower costs per kWh for the active material used and is therefore a highly probable scenario, especially with regard to the cost situation for battery materials. The recovery of manganese from active materials has so far been carried out in the research work mainly by means of solvent extraction, whereby this process entails many technological prerequisites in addition to the high price of the technique itself. When classical precipitation methods using sodium hydroxide or carbonate were used alternatively, only an inconsistent product with a high content of impurities could be obtained. This research work therefore deals with the selective recovery of manganese by means of photocatalytic oxidation. It makes utilization of the natural oxidation cycle of manganese, which is strongly dependent on the pH value, and shows that the efficiencies of this process are quite promising for the application in the field of battery recycling.

Keywords: Recycling, Lithium-Ion Batteries, Manganese Recovery, Photocatalytic Oxidation

1. Introduction

The importance of lithium-ion-batteries (LIBs) for today's and future society is undisputed, especially when considering the advancing climate crisis and the European Union's commitment to battle it by transforming today's fossil based economy to a net carbon zero one by the year 2050 [1]. This undertaking requires major changes in most industrial sectors, many of them relying on LIBs as their substitute energy source, including the world's automobile manufacturers. However, studies show that EVs often have a similarly negative impact on the environment like fossil fuel-based transportation, because approximately 20% of the total energy consumption of an EV-battery's lifetime can be traced back to its manufacturing process from primary raw materials. The recycling of LIBs and the use of secondary raw materials for the production of new LIBs can potentially reduce the footprint up to 40% [2]. The growing effort to reuse and recycle is also caused by the EU's goal to reduce its dependence for critical raw materials, many of which are necessary for the production of LIBs. [3]

2. Literature Review

The term lithium-ion battery refers to secondary batteries with lithium-ions acting as electrical charge carriers. In general, they are made up of four main components: cathode,

anode, electrolyte, and separator. Both anode and cathode are covered with active materials. Cathode active material accounts for the largest fraction of the battery of up to 43 wt-%. Therefore, it is characteristically used to define a battery. [4, 5]

Among a broad variety of different LIB types that are in application today, but for the use in EVs, NMC (Nickel-Manganese-Cobalt)-batteries are mainly employed with an approximated market share of 80%, expected to reach 90% before 2030. The NMC-chemistry however is constantly evolving with the goal to minimize the Co- by increasing the Ni-content. This is possible due to their similar chemical properties and 86% of Europe's cobalt supply is dependent on the import of raw materials from the Democratic Republic of Congo. While NMC 111 and 622, with the numbers displaying the ratio of metal masses (Ni:Mn:Co), are predominant in 2020, NMC 811 and 9.5.5 batteries will overtake until 2035. Further developments of batteries towards higher nickel contents are always aimed at extending the range of EVs, but also bring some challenges with them such as thermal instability and short lifetimes among others. [3, 6]

According to studies, the demand for LIBs will rise approximately 1,700% until 2025 (starting from 2019), passing 3,600 GWh, while the market for the recycling and reuse of spent LIBs in the European Union will grow to 850 million € until 2030. This steep rise will mainly be driven by the automobile sector as 85% of new LIBs in 2025 will be used in electric vehicles, according to data gathered by the Global Battery Alliance, the World Economic Forum, and McKinsey & Company. [7, 8]

Another prognosis released by the World Bank predicts an increase in demand for the relevant battery materials Al, Co, Fe, Pb, Li, Mn, and Ni by 1,000% until 2050 when pursuing the 2°C-climate-change target. Specifically, manganese can also be identified as an important raw material for battery production. High-purity manganese products are important raw materials and the declaration refers to a range of highly refined end products that are essential for most lithium-ion batteries. Europe, North America, Japan, Korea and many other countries import 100% of their manganese requirements, including high purity electrolytic manganese metal (HPEMM) and high purity manganese sulphate monohydrate (HPMSM), which are essential raw materials used in the production of lithium-ion EV batteries. The demand for high-purity manganese will therefore increase at least at the same rate as battery production. The composition of a classic lithium-ion battery and the associated costs for the raw materials can be seen in Figure 1a. It shows that currently manganese still plays a subordinate role in terms of costs. Depending on the battery type and the composition of the cathode material, different amounts of manganese are required. However, since four important EV manufacturers (including Tesla, Volkswagen, Stellantis and Renault) are developing high-manganese lithium-ion batteries, this is causing a major upward revision of the demand projection forecasts for high purity manganese. A massive increase in manganese consumption from 37,000 tonnes in 2020 to up to 900,000 tonnes in 2030 is expected (see Figure 1b). [3, 9]

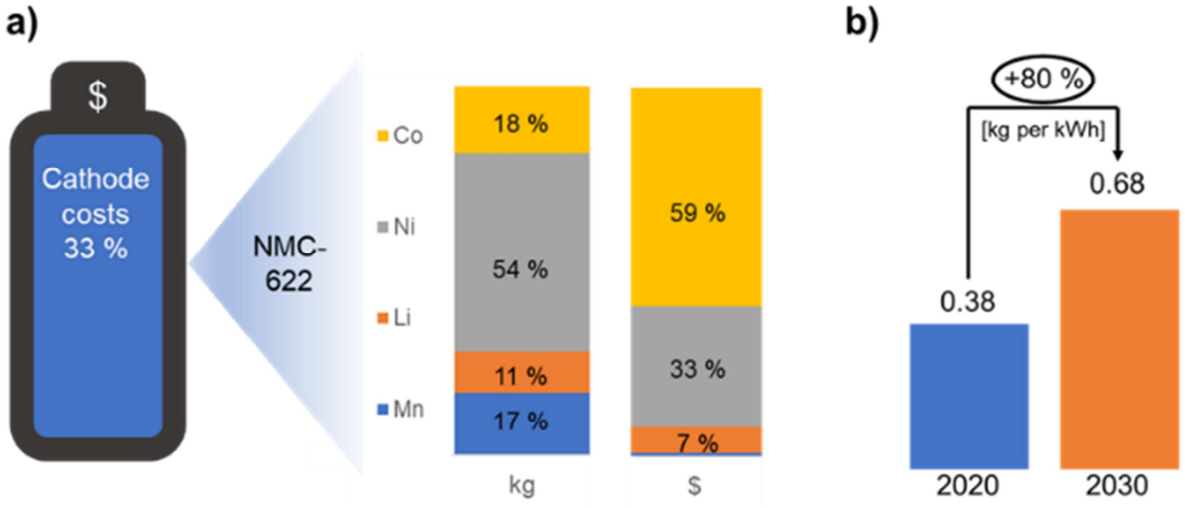

Figure 1. *(a) Nickel-manganese-cobalt (NMC) cathode batteries and corresponding distribution of the elements in mass and cost share (b) Increasing high purity manganese requirement 2020 to 2030 (average in EU) [9].*

Europe has become a major global producer of EVs in recent years, which means that the battery industry also needs to evolve. With seven battery cell gigafactories (> 1 GWh/annum of battery production), Europe relies on a development towards cheaper and more environmentally sustainable cells. Figure 2 shows the dependence of NMC production on high-purity manganese and also links this to corresponding costs, which explain the move towards high-manganese cells. [9]

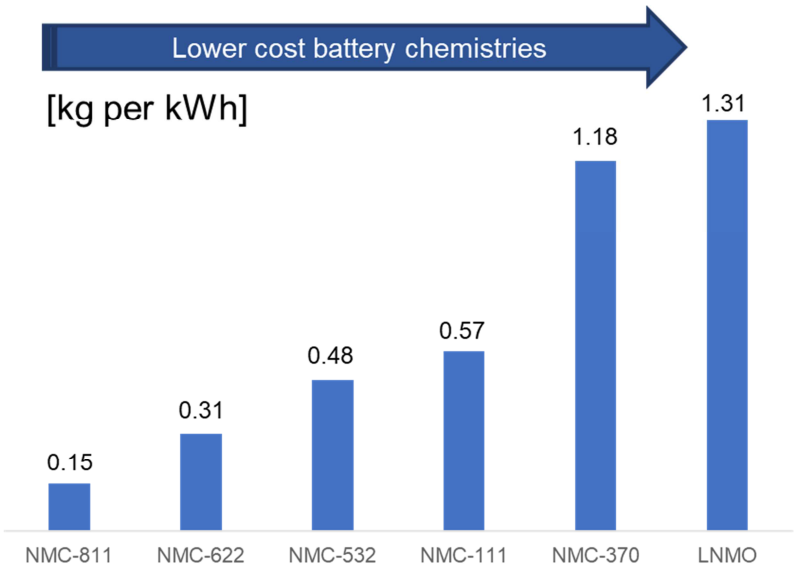

Figure 2. *High-purity manganese requirement by battery chemistry [9].*

Within the European Union, the collection, reuse, and recycling of lithium-ion-batteries are regulated by the Directive 2006/66/EC on batteries and accumulators, or "Batteries Directive". In 2019, however, after evaluating the directive, criticism arose claiming this regulation is outdated. Therefore, in December 2020, a first new draft for a new Batteries Directive was released by the European Commission. It takes the rapidly growing sector of electromobility into account and mentions ambitious recycling rates for batteries. Manganese, however, still remains mostly unmentioned. Although only about 5 wt-% of the material that can potentially be recycled in NMC batteries is Mn, the absolute numbers show that vast quantities of residues from the primary production could be avoided by recycling. [10-12]

Although 90% of manganese produced today is used in the steel industry, with the rapidly growing demand for LIBs and especially NMC-batteries, high quality "battery-grade" Mn will increasingly be needed in the electromobility sector. [12, 13]

A working group of the Batteries Europe (European Technology and Innovation Platform) released the first version of a raw materials and recycling roadmap in 2018. It aims to provide stakeholders with the necessary information to make strategic mid- and long-term decisions to lower the EU's dependence on raw material imports. This roadmap focuses on the sourcing of secondary raw materials through the collection and recycling of spent LIBs. It states that metallurgical processes for the recovery of the contained elements need to evolve to make Li, C, Mn, Al, F, and P recyclable in the future. To reach these goals, milestones for the next 0–5 respectively 5–10 years were defined by the working group with the recovery of manganese being first priority of the long-term milestones. [14]

LIBs can be recycled either mechanically to recover compounds to directly reuse them in the production of new batteries or via a hydrometallurgical or pyrometallurgical recycling process to recover chemicals. Today, pyrometallurgical recycling methods that primarily focus on the recovery of Co and Ni are dominant. However, their efficiencies are lower compared to hydrometallurgical routes and to reach future recycling rates, the implementation of a hydrometallurgical recycling system will be necessary. [2]

In the future most LIBs will be used in EVs. This offers the major advantage that a collection system for scrap cars is already in place and can easily be extended to include used batteries. Broad research was conducted to identify the demand for battery materials for the EV-industry in the EU until 2050, presuming the pursuit of the Paris Agreement and the dominance of NMC batteries for electric cars. Because of the rapid growth in consumption, only between 1.6 and 7% of Mn demand can be met by recycling material, increasing to up to 24.7% until 2050, but this saves up to 4.25 million tons of solid residual waste and 1.42 million tons of waste water from the primary production. [12]

Today's approaches to selectively recover Mn from cathode material usually use solvent extraction or ion exchange resins. Both hydrometallurgical separation methods involve expensive materials that can soon exceed the economic value of Mn. However, redox reactions involving Mn are major drivers of the electron flow in nature. The oxidation of Mn^{2+} (aq) in nature and the catalytic effects of UV-light, other dissolved elements, solid minerals, or microorganisms on the reaction has been studied, but mainly for geological and biological research. [15-19]

The photocatalytic oxidation of aqueous Mn^{2+} leached from cathode active material of spent NMC batteries could be an economically feasible method to selectively precipitate manganese from Co, Ni, and Li containing solutions on an industrial scale. As the element manganese, which is currently not yet classified as critical, is hardly recovered from spent lithium-ion batteries at present, the development of an efficient recycling process enables strategic independence from external raw material supplies as well as the closing of raw material cycles.

In principle, ultraviolet light has the ability to induce electron transfer reactions far from thermodynamic equilibrium and thus to change the oxidation state of metals. This is particularly evident on the Earth's surface, where light is the primary source of energy for the oxidation of molecules. The photochemical reaction of manganese can be described by the transition of Mn(II) to Mn(III), where this reaction has a redox potential of -1.54 V. Values for the band gap of $MnCO_3$ can be found representative in the literature. This is about 5.0 to 5.8 eV, indicating it can participate in photochemical reactions. By using UV light in a low wavelength range of 215 to 250 nm, precipitation can be realized by the wavelengths shorter than the absorption threshold. In the absence of oxygen, manganese oxyhydroxide is produced as well as H_2 (see equation (1)). [20–22]

$$2\,MnCO_3 + 4H_2O \overset{h\upsilon}{\rightarrow} 2\gamma - MnOOH + H_2 + 2HCO_3^- + 2H^+ \quad (1)$$

Basic thermodynamic data, indicates an endothermic reaction in which energy from light or heat is required. The supply of UV light at 230 nm enables the course of the reaction by the introduction of 520 kJ/mol. The production of H_2 proceeds in parallel with the formation of a solid phase and, according to the literature, reaches a plateau over time. This can be explained by the limitation of the photooxidation reaction. This reaction can only partially precipitate manganese, since it is limited by the surface area exposed to photons and water. Manganese oxyhydroxide is not stable and this compound is known to disproportionate in MnO_2 and Mn^{2+} under acidic conditions (see equation (2)). [20–22]

$$2\gamma - MnOOH + 2H^+ \leftrightarrow MnO_2 + Mn^{2+} + 2H_2O \quad (2)$$

MnO_2 is solid and can be seen as a brownish precipitate. This provides a plausible mechanism for the formation of higher valent manganese oxide by the supply of UV light only. [19]

From these reactions, the so-called manganese cycle can be assembled. This describes the oxidation states of manganese found in nature. Mn(II) is thermodynamically stable in the absence of O_2 and at low pH, whereas in the presence of O_2 Mn(III) and Mn(IV) are favored, occurring mainly as insoluble Mn (oxhydr)oxides (see Figure 3).[20–22]

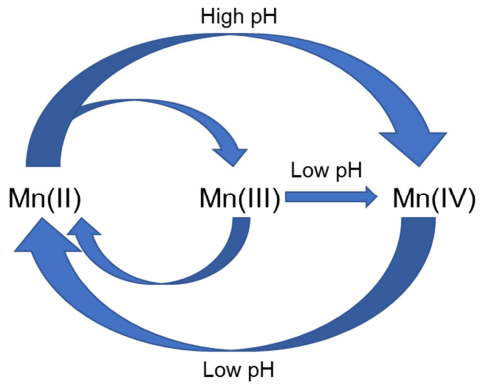

Figure 3. *Manganese cycle of oxidation states found in nature. [22]*

Within the scope of this research work, the principle possibility of precipitating manganese by means of UV light from aqueous solutions of hydrometallurgical LIB recycling is to be evaluated. This can be realised by means of a test series with the aid of a statistical experimental design and evaluation in order to verify the results obtained.

3. Materials and Methods

To investigate the effects of UV-light on Mn^{2+} ions in aqueous solutions, pure chemicals were used in this stage of research instead of leached battery active material to exclude side effects due to impurities.

In order to test and quantify the photocatalytic effect on manganese compounds, pH-adjusted solutions were left at different rotation speeds of the sample vessels in a darkened sample room under the influence of short-wave UV light for different durations. Glass sample vials with a capacity of 10 ml were used. These were placed in a specially manufactured sample plate with a defined average distance of 15 cm from the UV lamp. A variation of the rotation speed between 0 and 60 rpm was selected. The wavelength of the ultraviolet light was kept constant at 256 nm for all experiments.

Pure laboratory chemicals in different concentrations were used to prepare the initial solutions. In order to observe a possible effect of the concentration gradient, starting solutions with 5, 10, 25 and 50 $g \cdot l^{-1}$ Mn were prepared from $MnSO_4 \cdot H_2O$ (> 98%, Carl Roth, Germany) as many leaching processes in the context of battery recycling work with sulphuric acid solutions and a composition as close to reality as possible was chosen here. For the adjustment of the desired pH value, a diluted ammonia solution (25%, Carl Roth, Germany) was used in order to avoid introducing foreign ions into the initial solution, which may change the influence of the UV light. The pH value of all initial solutions was adjusted to pH=8–8.5, as the recovery of manganese in the field of hydrometallurgical battery recycling should also take place in this range.

After preparation, the solutions were immediately transferred to the sample vials and placed in the darkened sample room so as not to be influenced by natural light sources. Furthermore, samples were taken for analysis for all initial solutions. After transferring the sample to the sample tray, the motor and the UV lamp were started and the darkened sample chamber was closed. After the appropriate irradiation time of the sample, it was removed from the sample holder and the formed solid residue was extracted from the solution by means of vacuum filtration (mesh size: 2–3 µm). The solids were dried at 105 °C for at least 24 hours and their morphology and composition were determined by EDS analysis on the Jeol JSM-IT300 scanning electron microscope (Freising, Germany). In addition, element mappings were taken to check the homogeneity and distribution of the individual elements. The residual concentration of manganese in the liquid was determined by atomic emission spectrometry with microwave-induced plasma (MP-AES, Agilent 4210).

In addition to the decrease in concentration of manganese,

the electrochemical potential and the pH value (measured with WTW ino Lab, pH 7110) before and after UV irradiation were also evaluated for all samples. The statistical experimental design and evaluation was carried out using the software Modde 12.1 (Sartorius AG, Goettingen, Germany). The parameters residence time, rotation speed and initial concentration of the manganese were used for the design of experiments. The corresponding experimental plan results in 20 individual experiments per each rotation stage (rotation speeds of 0, 30 and 60 rpm were tested). The corresponding samples were removed from the sample set-up after 24, 48, 96, 168 and 336 hours and treated accordingly. The temperature was kept constant for all experiments at 25°C.

In classic hydrometallurgical recycling processes for spent lithium-ion batteries, manganese is usually separated in one of the last steps by solvent extraction or removed by means of precipitation processes. Since the former is mainly characterized by the high expense and the latter often only allows impure precipitates, the tested process should enable selective precipitation of the manganese and a high-quality product. In order to do justice to the process chain, lithium ions in the form of $LiSO_4 \cdot H_2O$ (10 $g \cdot l^{-1}$; 99%, Acros Organics, Janssen Pharmaceuticalaan) is deliberately added to defined solutions in order to simulate real process conditions and to check the possible influence of the dissolved lithium.

4. Results and Discussion

In the first step, an evaluation of the results of non-moving samples takes place in order to be able to draw a comparison to the rotating samples. The investigations focus on the remaining manganese content in the solution after different irradiation durations of the samples. Figure 4 shows the relative decreases in manganese concentration after 168 and 336 hours, as a decrease due to the photocatalytic oxidation of Mn(II) can be assumed after this time and enables a representative evaluation of the liquid samples. This primary experiment was carried out for all initial concentrations of the subsequent test ranges in order to be able to assess possible influencing factors such as the concentration gradient already at this stage of research.

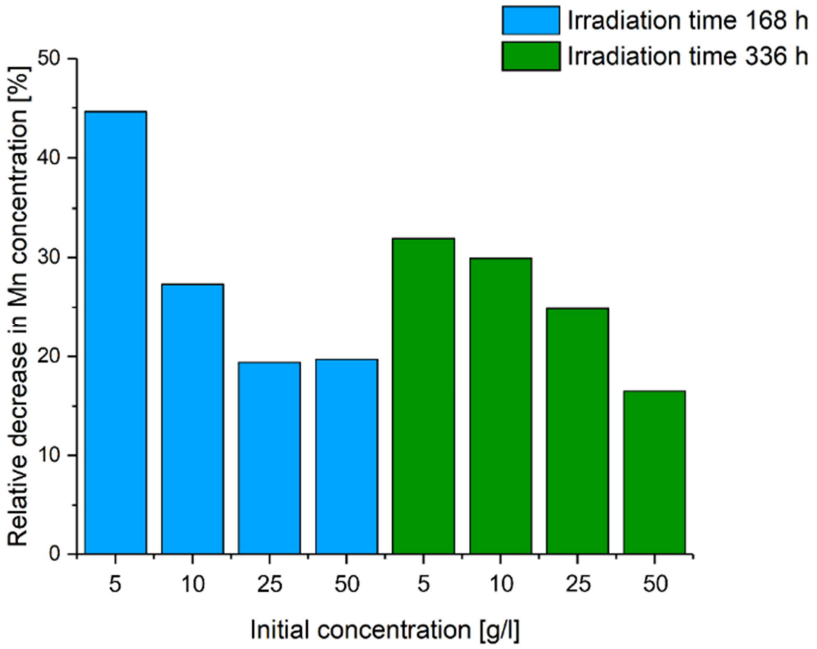

Figure 4. *Relative decrease in Mn concentration as a function of irradiation duration and initial concentration.*

On the one hand, this diagram shows that the initial concentration has a clear influence on the relative decrease of the Mn concentration after a defined irradiation period. This can be explained by the lower number of manganese ions in relation to the same amount of energy introduced. Since this is significantly higher in relation to the lowest initial concentration of 5 $g \cdot l^{-1}$ than at an initial concentration of 50 $g \cdot l^{-1}$, a more pronounced photocatalytic reaction also occurs. This can be demonstrated by a relative decrease of 45% after 168 for an initial concentration of 5 $g \cdot l^{-1}$ and just under 35% after 336 hours for 50 $g \cdot l^{-1}$, respectively. Lower yields were achieved for all other starting concentrations.

In the following section, the evaluation of the rotating samples is carried out, especially with regard to the influence of the rotation speed.

As shown in Figure 5, it is not useful to look at the absolute residual concentrations of manganese in the solution, as the differences in the concentration decreases are difficult to summarize. For this reason, the relative decreases of the manganese concentration in the solutions are examined more closely. Furthermore, the EpH value was measured both before and after the defined irradiation period and showed an increase of approx. 200 mV for all samples as well as a decrease of the pH value to < 7.40 for all samples. As shown in figure 6, the samples with a rotation speed of 30 rpm show relative decreases in concentration between 1.79 and 30.38%

depending on the initial concentration as well as the duration of the irradiation. It can be seen that higher initial concentrations do not necessarily lead to higher concentration gradients. The most promising results were obtained at samples with an initial concentration of 10 $g \cdot l^{-1}$ Mn, whereby the maximum of 30.38% was achieved after a test period of 96 hours. Longer irradiation periods of 168 or 336 hours again led to significantly poorer precipitation results. This can be explained by the dissolution of already precipitated manganese during the Mn cycle. Due to the lowering of the pH value, which could be observed over the duration of the experiment, Mn can redissolve again as Mn (II) and is thus also present in the residual solution and cannot be detected as precipitated solid. However, this behaviour is mainly visible at lower concentrations, while solutions with higher initial concentrations are not yet at this stage of the Mn cycle and the best results were also obtained after the maximum test duration of 336 hours. With an initial concentration of 25 $g \cdot l^{-1}$ Mn, a relative decrease of 10.81% could be achieved after 336 hours, and with 50 $g \cdot l^{-1}$ Mn, 27.09%, respectively. These values do not represent the absolute peak values, since due to the high manganese concentrations in the initial solutions, high amounts of energy must be introduced to enable precipitation of the manganese as Mn (IV).

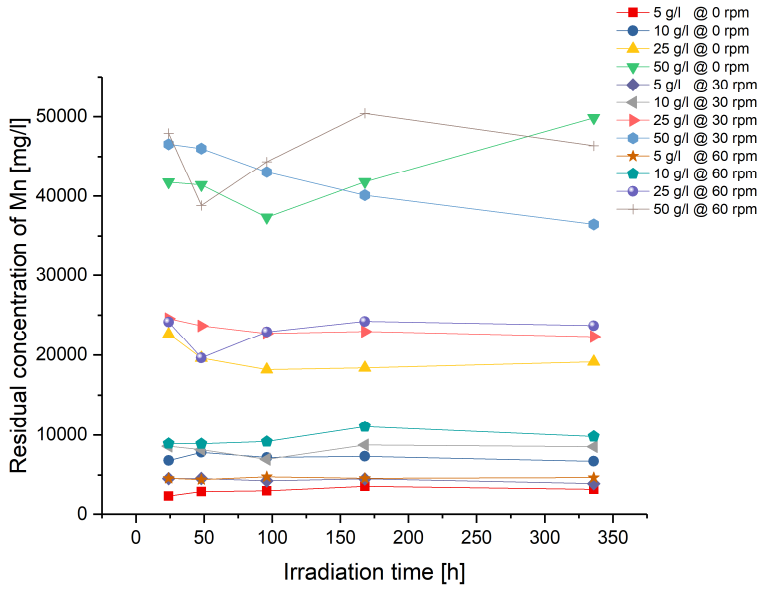

Figure 5. *Concentration profils of all initial solutions as a function of the rotational speed and irradiation duration.*

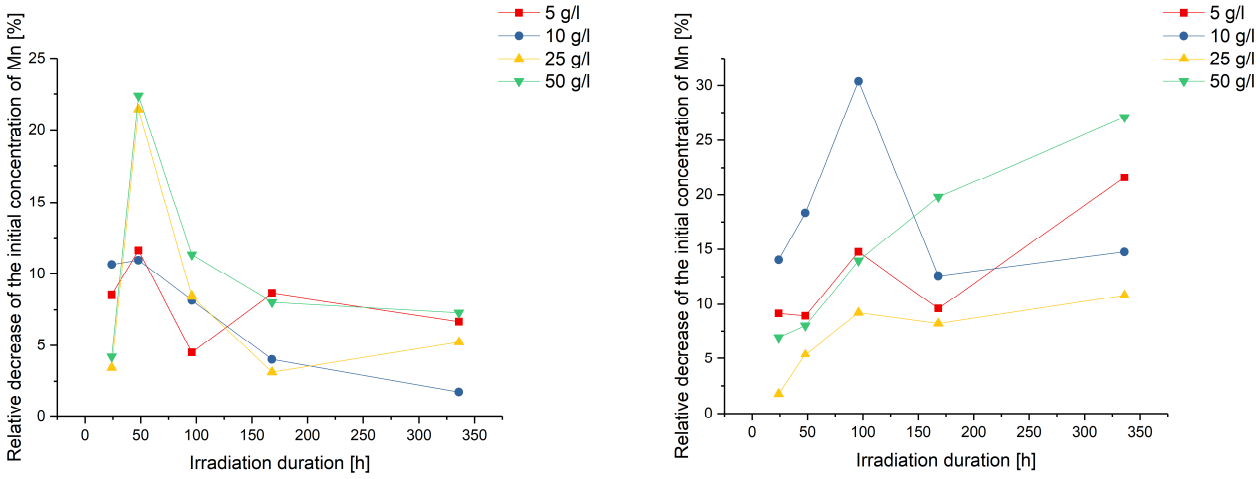

Figure 6. *Relative decrease of the inital concentration of Mn as a function of irradiation duration and a rotational speed of (a) 30 rpm and (b) 60 rpm.*

The series of tests at a higher rotation speed of 60 rpm and the same initial concentrations prove a clear influence of this changed parameter. After 48 hours of irradiation, the higher-concentration starting samples give the best results, with a decrease in Mn concentration of up to 22.37%. Low-concentration initial samples (respectively 5 and 10 $g \cdot l^{-1}$) also show the best results after this experimental period, but at a much lower level between 10.97 and 11.64% of decrease. This suggests that, on the one hand, the increased rotation speed leads to a shortening of the necessary

irradiation time to achieve the same results in terms of relative decrease of Mn concentration and, on the other hand, the manganese cycle is accelerated as a result. After reaching these maxima, clearly worse precipitation results can be seen for all samples, which suggests that, due to the decrease in pH, redissolution processes are already taking place as part of the manganese cycle. The measurement results of the pH samples confirm a decrease of the pH values to < 6.46. This value is clearly below the maximum value of the samples with a rotation speed of only 30 rpm. It can thus be demonstrated that the higher rotation speed of the samples allows better mixing as well as more uniform irradiation of the samples by the UV lamp, thus accelerating the manganese cycle. In return, however, it should be noted that if the pH falls below specific values, this also leads to more rapid redissolution of the precipitated manganese into the initial solution, and the process should therefore be subject to defined control.

From the data obtained for pH values, EpH values and Mn concentrations, a statistical model was created using the experimental design and evaluation program Modde 12.1. On the one hand, this provides the possibility of investigating a parameter field and, on the other hand, the clear presentation of the results as a function of the output variables. This model is to be used for future estimations as well as the choice of the optimal parameter field.

Figure 7 shows the decrease in manganese concentration in the aqueous solutions as a function of rotation speed as well as irradiation time. This representation is based on a full-factorial model with 40 individual experiments, in which interactions of the influencing parameters were also taken into account. The parameters irradiation period, rotation speed of the samples as well as the initial concentration of the solutions were varied.

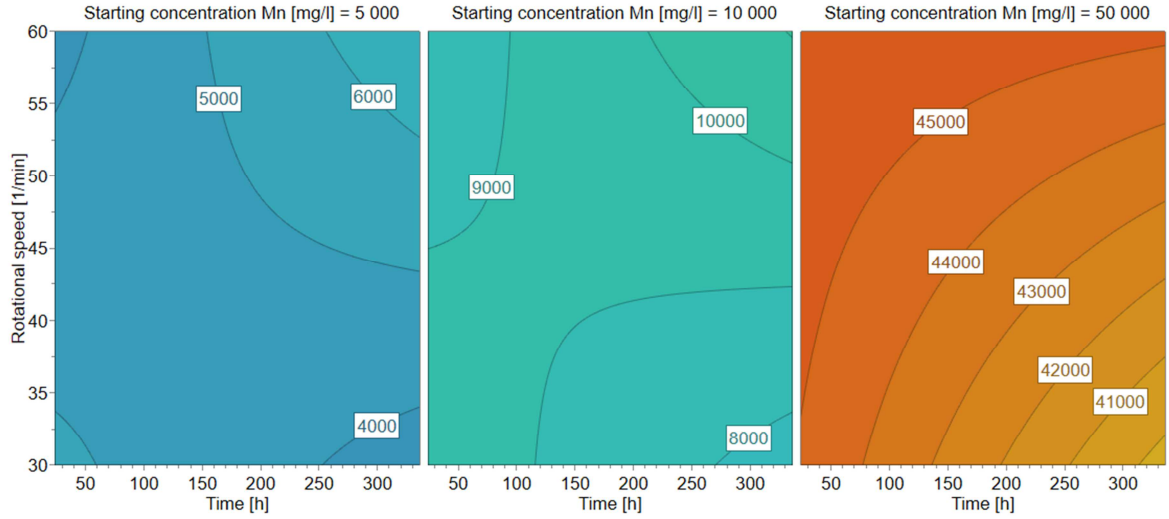

Figure 7. *Statistical experimental evaluation of the residual manganese concentrations in the solution as a function of the rotational speed and the irradiation time.*

The coefficient of determination R^2 and the predictive power Q^2 represent key figures in statistics that describe the quality of a regression. R^2 is used to evaluate how well the measured values fit a model. Meanwhile, Q^2 represents the predictability of an unknown value. For the evaluation using the response manganese concentration, a coefficient of determination of 0.984 and a predictive ability of 0.938 were obtained. This shows that the model delivers quite reliable forecasts and has a high coefficient of determination.

It is shown that at low initial concentrations, irradiation durations of 180 hours at 30 rpm are necessary to achieve a reduction of the original concentration by 12.5%. Furthermore, the model indicates that high rotation speeds lead to similar results for short irradiation durations (<100 h). This can again be explained in the context of the Mn cycle. Higher durations at rotation speeds above 45 rpm statistically lead to a significant deterioration of the process. In this case, a statistical error occurred during the evaluation, since according to the model more than 5,000 $mg \cdot l^{-1}$ Mn could be present in the solution. This is, of course, not possible in reality, since at maximum the initial concentration of 5,000 $mg \cdot l^{-1}$ can be existent in the aqueous solution.

Similar tendencies can also be observed at an initial concentration of 10 $g \cdot l^{-1}$, whereby the maximum concentration decreases could be detected at a long irradiation time (>250 h) and low rotation speeds. A massive increase of the Mn concentration in the starting solutions shows a changed picture. Here, only long irradiation durations and low rotation speeds lead to a significant decrease in the Mn concentration in the solution. Higher rotation speeds of > 30 rpm showed poorer results over the entire sampled period. This is related to the high Mn concentration compared to the other solutions tested. Since the same UV source was used for all tests, it can be assumed that the same energy was always applied to the samples. Due to the high manganese concentration, the effective precipitation takes longer and no decrease of the pH values and thus a progress of the Mn cycle can be detected. This shows a dependence on the initial concentration of the solutions as well as on the rotation speed of the samples in the test.

The effect of the initial concentrations on the effectiveness of UV precipitation within 336 hours just explained can also be clearly seen from the recordings and the model created as a function of the pH value (see Figure 8). At lower starting concentrations, similar irradiation durations as well as rotation speeds give almost identical results with regard to the pH value. This effect changes significantly at high starting concentrations. It can be seen that the rotation speed exerts less influence and the irradiation duration significantly more. This also corresponds to the underlying assumptions regarding the Mn cycle.

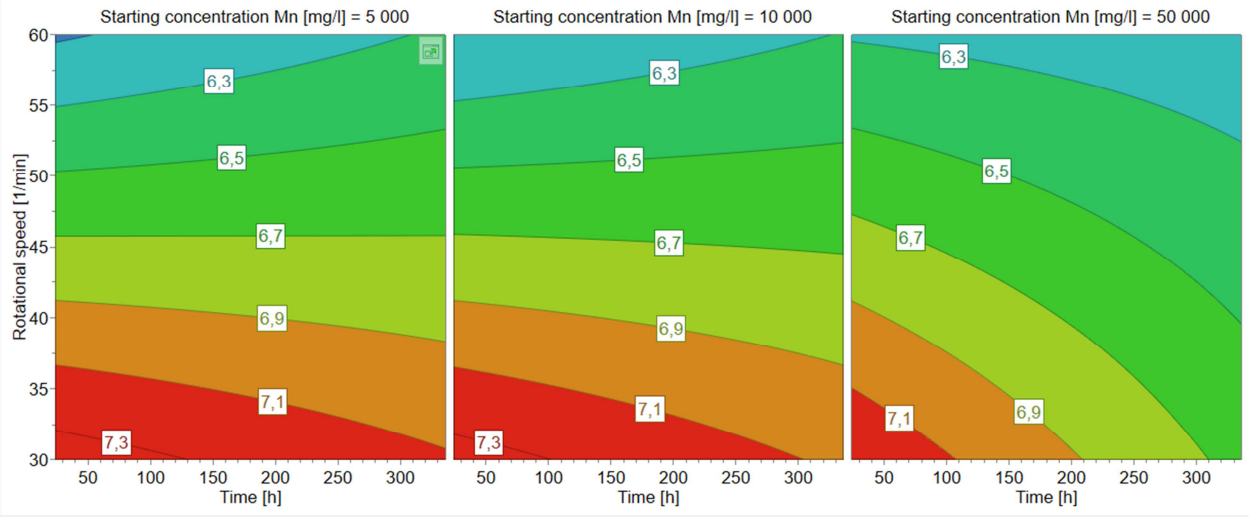

Figure 8. *Statistical experimental evaluation of the pH value after the experiment as a function of the rotational speed and the irradiation time.*

The described effect can be illustrated even more clearly by evaluating the measured EpH values. The EpH values of the initial solutions lay in a range between 89 and 124 mV and thus in a quite narrow parameter window. After a defined irradiation period, an increase of at least 40% in the EpH value was observed for all tests, whereby a significantly higher increase was recorded for the majority of the samples (see Table 1).

Table 1. *pH and EpH values for all conducted experiments before and after defined irradiation duration.*

Irradiaton time	Rotational speed	Starting conc.	pH before exp.	pH after exp.	EpH before exp.	EpH after exp.
[h]	[rpm]	[mg·l^{-1}]	[-]	[-]	[-]	[-]
24				7.40		7.40
48				7.40		7.40
96	30	5	8.47	7.61	8.47	7.61
168				7.48		7.48
336				7.14		7.14
24				7.19		7.19
48				7.24		7.24
96	30	10	8.33	7.27	8.33	7.27
168				7.12		7.12
336				6.86		6.86
24				7.32		7.32
48				7.30		7.30
96	30	25	8.13	7.39	8.13	7.39
168				7.06		7.06
336				6.93		6.93
24				7.26		7.26
48				7.18		7.18
96	30	50	8.00	7.18	8.00	7.18
168				6.91		6.91
336				6.75		6.75
24				6.02		214.30
48				6.17		212.00
96	60	5	8.72	6.18	89.80	195.90
168				6.11		192.40
336				6.43		202.20
24				5.95		213.20
48				6.20		210.50
96	60	10	8.51	6.28	101.60	189.50
168				6.14		187.60
336				6.30		188.00

Irradiaton time	Rotational speed	Starting conc.	pH before exp.	pH after exp.	EpH before exp.	EpH after exp.
24				6.09		180.50
48				6.21		183.10
96	60	25	8.11	6.15	122.30	181.60
168				6.14		176.10
336				6.23		174.30
24				6.46		166.20
48				6.22		170.40
96	60	50	8.06	6.29	113.90	168.10
168				6.16		167.90
336				6.19		160.10

At high initial concentrations of 50 $g \cdot l^{-1}$ Mn, the smallest increase in the EpH value was observed, which also corresponds to the results discussed so far, as it can be seen in Figure 9.

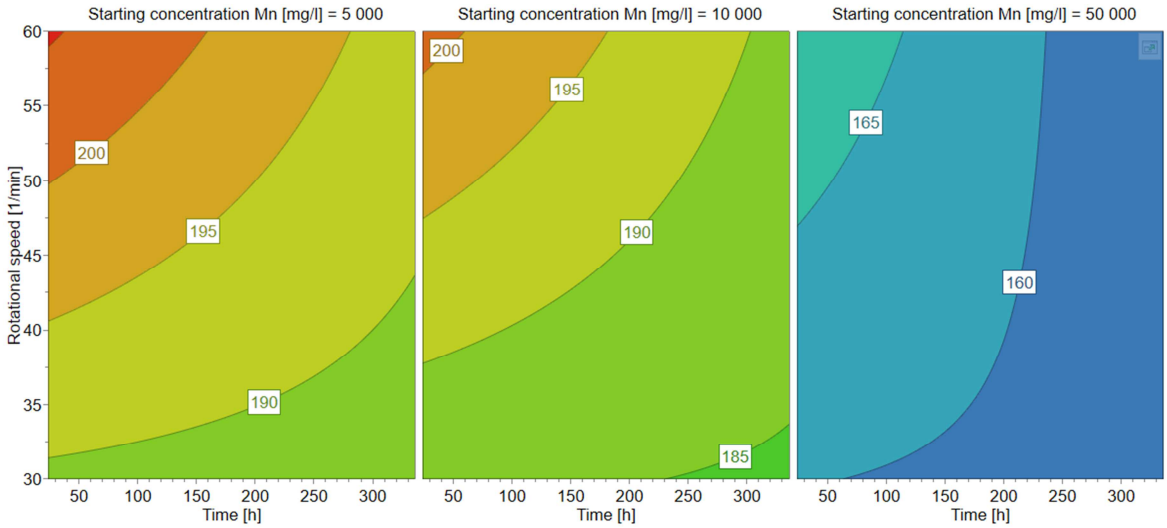

Figure 9. *Statistical experimental evaluation of the EpH value after the experiment as a function of the rotational speed and the irradiation time.*

Based on previous studies [15, 16] that dealt exclusively with the photocatalytic precipitation of manganese, these results show that the presence of foreign ions (e.g. Li^+) does not inhibit this effect. Due to the few publications that dealt with this topic, new insights could be gained with regard to the influence of the rotation speed and irradiation time.

The precipitated Mn-containing product was characterised by SEM/EDS and it was shown that a platy structure of the MnO_2 particles occurs in this configuration as shown in Figure 10, with the manganese evenly distributed throughout the filter cake. This statement is also confirmed by the corresponding element distribution. Furthermore, sulphur can be detected on the filter cake, whereby this originates from the sulphuric acid solution and only represents a build-up, since the product obtained was not washed with distilled water. The sulphur content of the filter cake was in the low single-digit percentages for all samples analysed. Figure 10 is representative of all analyses of the products obtained, as both the morphology and composition provided very similar data and images for all samples.

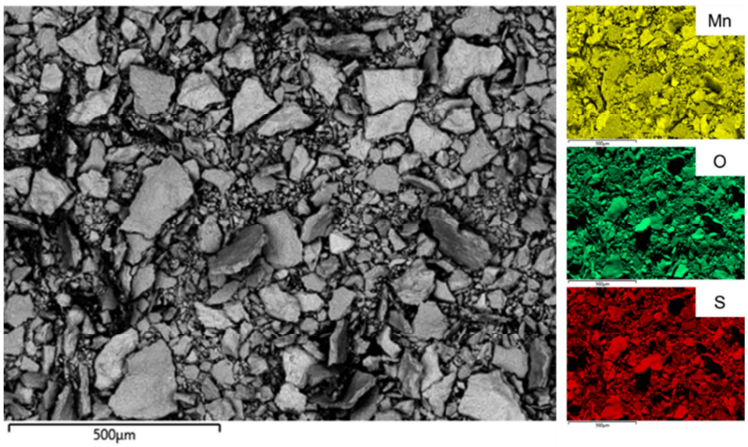

Figure 10. *SEM/EDS images and elemental distribution of the product obtained from the photocatalytic precipitation of MnO_2.*

5. Conclusion

Based on the results obtained, promising trends can be concluded for the recovery of manganese from aqueous solutions by means of UV irradiation. It was shown that both the irradiation time and the rotation speed and, above all, the initial concentration of the solution are essential parameters. With low initial concentrations, promising results could already be achieved with average irradiation durations of approx. 150 hours, but only at increased rotation speeds (>45 rpm). On the one hand, this can be attributed to the mixing and uniform irradiation of the samples, but also to the clear increase in the EpH value as a function of the duration and the rotation speed. This increase is also followed by a drop in the pH value, which at high rotation speeds and long irradiation durations leads to negative effects such as a redissolution of the manganese already precipitated as Mn(IV) as Mn(II) in the solution. To avoid this behaviour, it is essential to work in the optimal parameter field. The described effect cannot be observed with higher concentrated initial solutions. This can be attributed to the significantly lower amounts of energy added in relation to the mass of manganese in the solution. Accordingly, there is also a significantly smaller drop in the pH values and a smaller increase in the EpH values. The evaluation of a full-factorial experimental model confirmed and visualised this hypothesis.

These results are a significant advance for the hydrometallurgical recycling of lithium-ion batteries, as there are still large amounts of manganese in the solutions after the recovery of cobalt and nickel, especially in precipitation-based processes. The UV-based precipitation method makes it possible to realise a residue-free and sustainable alternative to classic precipitation methods, e.g. using sodium hydroxide or sodium carobonate. Furthermore, this method enables selective recovery of the high-quality manganese. Although the basic research presented in this publication is based on synthetically produced solutions, it shows in principle the promising possibilities offered by this alternative precipitation method, especially in the context of the manganese cycle. For the future, the corresponding test series must be carried out and verified with authentic leaching solutions in order to study possible influences by foreign ions in the aqueous solutions.

References

[1] European Union: European Commission: The European Green Deal, Brussels (2019).

[2] Larouche F. et al.: Progress and Status of Hydrometallurgical and Direct Recycling of Li-Ion Batteries and Beyond. Materials (Basel, Switzerland), 13 (2020) online proceedings.

[3] Widerstandsfähigkeit der EU bei kritischen Rohstoffe: Einen Pfad hin zu größerer Sicherheit und Nachhaltigkeit abstecken, Mitteilung, Brüssel (2020).

[4] Leuthner S.: 2 Lithium-ion battery overview. In: Korthauer, R. (Hg.): Lithium-Ion Batteries: Basics and Applications. Berlin, Heidelberg: Springer Berlin Heidelberg; Imprint: Springer, 13–20.

[5] Arnberger A., E. Coskun und B. Rutrecht: Recycling von Lithium-Ionen-Batterien. In: Sammelband. Thiel, S., Thomé-Kozmiensky, E., Goldmann, D. (Hg.): Recycling und Rohstoffe. Neuruppin: Thomé-Kozmiensky Verlag GmbH, 583–599.

[6] Lithium, Cobalt and Nickel: The Gold Rush of the 21st Century. Daraday Insights (2020) online proceedings.

[7] McKinsey & Company: Powering up sustainable energy, Bericht (2020).

[8] Global Battery Alliance, World Economic Forum: A Vision for a Sustainable Battery Value Chain in 2030, Bericht, Geneva, Schweiz (2019).

[9] Votava, J.: Euro Manganese Inc. Internet: https://www.mn25.ca/manganese (Access: 25.03.2022).

[10] Europäische Kommission: Batteries and accumulators. Internet: https://ec.europa.eu/environment/topics/waste-and-recycling/batteries-and-accumulators_en (Zugriff: 21.06.2021).

[11] Halleux V.: New EU regulatory framwork for batteries, Bericht, Brüssel (2021).

[12] Xu C. et al.: Future material demand for automotive lithium-based batteries. Communications Materials, 1 (2020) online proceedings.

[13] Schnebele E.: Manganese Statistics and Information. Internet: https://www.usgs.gov/centers/nmic/manganese-statistics-and-information (Zugriff: 18.10.2021).

[14] Kauranen P. et al.: Raw Materials and Recycling Roadmap (2021).

[15] Anbar A. D. und H. D. Holland: The photochemistry of manganese and the origin of banded iron formations. Geochimica et Cosmochimica Acta, 56 (1992), 2595–2603.

[16] Diem D. und W. Stumm: Is dissolved Mn^{2+} being oxidized by O_2 in absence of Mn-bacteria or surface catalysts? Geochimica et Cosmochimica Acta, 48 (1984), 1571–1573.

[17] Jung H. et al.: Photocatalytic Oxidation of Dissolved Mn^{2+} by TiO_2 and the Formation of Tunnel Structured Manganese Oxides. ACS Earth and Space Chemistry, 5 (2021), 2105–2114.

[18] Euro Manganese Announces PEA Results for Chvaletice Manganese Project with an after-tax Net Present Value of US$593 Million, Vancouver, Canada (2019).

[19] Keller A., M. W. Hlawitschka und H.-J. Bart: Manganese recycling of spent lithium-ion batteries via solvent extraction. Separation and Purification Technology, 275 (2021), 119166.

[20] Liu, W. et al.: Anoxic photochemical oxidation of manganese carbonate yields manganese oxide. In: Proceedings of the National Academy of Sciences 117, 37 (2020), 22698– 22704.

[21] Yamaguchi, K. et al.: The Redox Chemistry of Manganese (III) and –(IV) Complexes. Israel Journal of Chemistry, 25 (1985), 164–176.

[22] Tebo, B. M. et al.: Biogenic Manganese Oxides: Properties and Mechanism of Formation. Annu. Rev. Earth Planet Sci. 32 (2004), 287–328.